PCCP

Accepted Manuscript

ROYAL SOCIETY OF CHEMISTRY

www.rsc.org/pccp

A facile synthesis of highly stable and luminescent Ag cluster: a steady-state and time-resolved spectroscopy study

Nabin Kumar Pal, Carola Kryschi*
Department of Chemistry and Pharmacy and ICMM, Friedrich-Alexander University of Erlangen-Nuremberg, Erlangen, Germany.
*Email: carola.kryschi@fau.de

Abstract

In this paper, we reported of a very simple and environmentally friendly procedure for the synthesis of bright luminescent and nearly monodisperse Ag nanoclusters stabilized by poly (N-vinylpyrrolidone) homopolymer. In this synthesis route acetonitrile or N,N-dimethylformamide (DMF) act as both, solvent and reducing agent at their respective reflux temperatures. The as-prepared Ag clusters were found to be highly stable in various solvents as well as show nearly no changes in their emission intensity in solutions with different pH values and ionic strengths. Remarkably, the acetonitrile method predominantly produces blue emitting Ag clusters with a photoluminescence (PL) emission maximum at 424 nm (quantum yield 3.5 %), whereas mainly blue-green emitting Ag clusters with the PL emission maximum at 450 nm (quantum yield 2.7 %) were formed using the DMF method. The photo-physical, electronic, structural and morphological properties of the Ag clusters were examined performing UV/Vis absorption spectroscopy, stationary and time-resolved PL spectroscopy, X-ray photoelectron spectroscopy, femtosecond transient absorption spectroscopy, and transmission electron microscopy experiments.

1. Introduction

Luminescent noble metal clusters are one of the most promising materials in nanoscience nowadays[1-8]. Clusters having a size of less than 2 nm behave like a bridging entity between atoms and bulk materials. Due to such ultrasmall sizes as being on the scale of the Fermi wavelength of the conduction-band electrons (*ca.* 0.7 nm) and thereupon, in the quantum confinement regime[9,10], noble metal clusters exhibit molecular-like electronic transitions between discrete energy levels and show new size-tunable optical and electronic properties[11,12,13]. Size-tunable properties, along with high photostability and low cytotoxicity, make these clusters an attractive candidate for versatile applications such as in optical

sensing[14-18], catalysis[19], bio-labelling[20,21], bio-imaging[22], single-particle optoelectronics[9], surface enhanced Raman spectroscopy[23] and others.

Among the noble-metal clusters gold clusters have been extensively studied over the past two decades. However, only a few synthesis techniques for the preparation of stable luminescent silver (Ag) clusters are known. In recent past, the research activities on Ag clusters have enormously increased and since then, various synthesis procedures have been developed to produce stable luminescent Ag clusters that are stabilized by a variety of protecting ligands. Among various methods, template-based synthesis techniques are the most recognized ones. Different kinds of templates such as polymers[19,24,25], proteins[26,27], DNA[21,28], oligonucleotide[29,30], polyelectrolyte[31], dendrimers[32,33], and polymer microgel[34] have been used so far. Small molecules, especially those containing carboxylic or thiol groups[35,36], were also utilized as stabilizers. Dickson and co-workers were the first who produced small Ag clusters by irradiating UV light onto a silver-oxide film[37]. Later on, the same group reported of highly stable and luminescent Ag and Au clusters incorporated in OH-terminated poly(amidoamine) (PAMAM) dendrimers in aqueous solution[32,33]. Martinez *et al.* [21,38] synthesized DNA-templated stable Ag clusters that were successfully applied for protein detection. Another novel synthesis procedure for bio-compatible, stable luminescent Ag and Au clusters was developed by Nienhaus *et al.*[39]. Recently Parak *et al.*[40] reported of a synthesis route that enable the preparation of water-soluble, red-luminescent Ag clusters with a mean size of 2.2 ±0.4 nm. In this sophisticated synthesis procedure didodecyldimethylammonium stabilized Ag nanoparticles with sizes around 4 nm were initially formed which were subsequently size-reduced by a ligand exchange process followed by heating and UV light exposure. Other routes such as radiolytic[41], microwave irradiation[42], sonochemical[43], electrochemical[44] methods have also been proven as useful to prepare noble-metal clusters.

However most of the methods mentioned above require photo-irradiation, electric field application or an external reducing agent such as sodium borohydride or ascorbic acid. In recent past Liz-Marzán and co-workers[45,46] could prepare noble-metal clusters by using N,N′-dimethylformamide (DMF) that was shown to act as both, mild reducing and stabilizing agent. Unfortunately these authors synthesized non-luminescent nanoparticles with sizes larger than 5 nm as being unambiguously obvious from the intense surface plasmon resonance absorption bands appearing in the visible. Later Liu *et al.*[47] extended this idea of using DMF as both, reducing and stabilizing agent, and they succeeded in developing a surfactant-free method allowing to synthesize highly stable and luminescent Au clusters which were

subsequently terminated with various ligands. However, in order to successfully synthesize these clusters using DMF, as reducing and stabilizing agent, the reaction mixture needs to be refluxed at a high temperature (153°C). The high boiling point of DMF makes the purification and drying process quite difficult.

In theory, the use of any solvent with a low boiling point and sufficient reducing ability may replace DMF in such reactions. We found out that acetonitrile is the solvent which matches those criteria and thus, can be employed for such reactions. Although, the use of acetonitrile failed for the synthesis of gold clusters, this solvent is very well suited for the preparation of highly stable, luminescent Ag clusters. Here we report of a facile route that was elaborated to synthesize luminescent Ag nanoclusters with sizes around 1.3 -1.5 nm, stabilized by poly(N-vinylpyrrolidone) (PVP, K30, M_w 40 KDa), where acetonitrile was used as both, solvent and reducing agent. This method needs a low refluxing temperature (75 ^oC in contrast to 153 ^oC for DMF). The low boiling point of acetonitrile considerably facilitates subsequent processing of the reaction products. The photoluminescence (PL) lifetime of the Ag clusters were found to be in the nanosecond (ns) time region. Furthermore, the ultrafast excited-states dynamics of the Ag clusters was studied by performing femtosecond (fs) transient absorption experiments utilizing 150 fs pump pulses at 387 nm and white-light probe pulses in the visible. The excited-states relaxation dynamics at short time scales (femtoseconds to picoseconds) were conceived to occur via ultrafast internal conversion (0.3 ps) from initially excited, higher lying electronic states to the longer-lived first excited (S_1) state and by trapping processes due to surface states.

2. Experimental Section

2.1 Materials

Silver nitrate (99.9999 % $AgNO_3$) was obtained from Sigma-Aldrich, Poly(N-vinylpyrrolidone) K30 (PVP; $(C_6H_9ON)_n$), M_w ~ 40 KDa) from Fluka, $NaBH_4$ (97%) Acetonitrile (LC-MS Chromasolv® ≥ 99.9%) from Fluka; N,N′-Dimethylformamide from Roth (≥ 99.8%), absolute ethanol and acetone (99.9%) from Merck, Membra-Cel® dialysis tubing (regenerated cellulose, MWCO 7KDa) from SERVA. All materials and solvents were used as received from the suppliers without further purification. In all syntheses milli-Q deionised water (18 MΩ) was used.

2.2 Synthesis of the Ag cluster

First, 0.075 M of poly (N-vinylpyrrolidone) (in terms of monomeric unit) was dissolved in 50 ml of acetonitrile in a three-necked round bottom flask fitted with a reflux condenser under argon atmosphere. The whole system was then placed on a heating plate in a silicon-oil bath and slowly heated, until the temperature reaches 75^{o}C. An aqueous solution of silver nitrate (0.5 ml of 0.1 M) was then added at once to this pre-heated solution under vigorous stirring. The reaction was allowed to proceed for at least 6 hours under reflux. In the mean time formation of the clusters can be checked by applying UV radiation ($\lambda_{max}\approx$ 364 nm) to the reaction mixture, from where a blue luminescence was observed which was getting more and more intensive with increasing refluxing time. Instead of acetonitrile, N,N´-dimethylformamide can also be used as both, solvent and reducing agent. This synthesis recipe yielded green luminescent Ag clusters. From now onwards we will designate the Ag clusters prepared using acetonitrile as A-AgPVP and the one prepared using DMF as D-AgPVP.

2.3 Purification of the Ag clusters

After the completion of the reaction the flask was allowed to cool down to room temperature. The reaction mixture was then centrifuged thrice at 12000 rpm for 30 min at room temperature (25^{o}C) to remove excess PVP and the larger nanoparticles. The supernatant obtained from this step was then evaporated to dryness under reduced pressure. The solid thus obtained was washed with an acetone/water mixture (v/v: 3/1) and then separated by centrifugation at 1000 rpm. This step was repeated several times, in order to remove the residual unbound polymer from the cluster solution. Finally the Ag clusters were dissolved in 3 ml of deionised water and then dialysed overnight using a cellulose ester membrane tube with a cut-off molecular-weight (MWCO) of 7 KDa in 100 ml of water.

2.4 Synthesis of Ag@PVP nanoparticles

Ag@PVP nanoparticles were synthesized by mixing 1 mM of $AgNO_3$ to 2 mM of PVP (in terms of monomeric unit) in 100 ml of methanol followed by adding freshly prepared 0.2 M of $NaBH_4$ in 20 ml of water under vigorous stirring. After 1 h stirring a dark brown precipitate was formed that was separated by centrifugation (8000 rpm for 15 min) at room temperature and then washed thrice with a water-methanol (20%) mixture followed by ethanol. After removing the excess solvent, finally a dark brown powder of the nanoparticle was obtained which shows the characteristic surface plasmon resonance peak at 397 nm in the absorption

spectrum. Though in this contribution the main emphasis will be given on AgPVP clusters, Ag@PVP nanoparticles have been synthesized only to give an insight to the difference in the sizes and optical properties between silver nanoparticle and silver clusters.

The as-prepared nanoparticles and also the clusters are easily soluble in water, methanol, ethanol and other protic solvents. For further characterization an aqueous solution of the nanoparticles and an ethanolic (absolute ethanol) solution of the clusters were used.

3. Methods

3.1 High-Resolution Transmission Electron Microscopy (HRTEM)

The HRTEM images were recorded using a Phillips CM 300 UltraTwin microscope. The measurements were carried out at an accelerating voltage of 300 kV in the bright-field mode. The TEM images were taken using a Zeiss EM 900 instruments operating at 120 kV accelerating voltage. The sample for the HRTEM and TEM were prepared by dropcasting 5 microliter of the ethanolic solution of the Ag nanoparticles and Ag clusters onto an ultrathin carbon coated copper grid (300 mesh) followed by drying in a vacuum at 25^{o}C for 2 days.

3.2 X-ray Photoelectron Spectroscopy

The chemical composition of the cluster was investigated with X-ray photoelectron spectroscopy (XPS, PHI 5600 XPS spectrometer). Monochromatic Al K_{α} was used as the X-ray source.

3.3 Steady-State Optical Spectroscopy

The PL spectra were recorded on a Jobin-Yvon FluoroMax-3 spectrofluorometer using the magic-angle polarization configuration and a slit width of 5 nm for both excitation and emission spectra. The UV/Vis absorption spectra were recorded on a Perkin Elmer UV/Vis absorption spectrometer Lambda 2. All experiments were performed at room temperature using quartz cuvettes with an optical path length of 10 mm.

The PL quantum yields of the Ag clusters were estimated using a fluorescence standard. The following relative comparison method was used to evaluate the quantum yield:

$$\frac{Q_t}{Q_s} = \frac{(I_t / A_t)\eta_t^2}{(I_s / A_s)\eta_s^2}\ , \qquad (1)$$

where Q is the PL quantum yield, I the integral area under the PL spectrum, η the refractive index of the solvent, and A the absorption at the selected excitation wavelength. The subscripts "t" and "s" represent the test sample and fluorescence standard, respectively.

3.4 Time-Resolved Optical Spectroscopy

PL decay profiles were recorded using the time-correlated single-photon counting (TCSPC) PL spectroscopy technique. This time resolved measurement of the PL intensity was carried out on the TCSPC spectrometer Fluorolog-3 (Jobin Yvon) equipped with a microchannel plate (Hamamatsu, R3809U-50) that provides a time resolution of about 60 ps.

Femtosecond transient absorption spectroscopy experiments were conducted with a Clark MXR CPA 2101 laser system in conjunction with an Ultrafast TAPPS HELIOS detection system, consisting primarily of a glass fiber based spectrometer. The output pulses at 387 nm with a 150 fs pulse and a 1 kHz repetition rate were used as pump pulses. They were obtained by amplifying and frequency doubling the 775 nm seeding pulses of the Er^{3+}-doped glass fiber oscillator in a regenerative chirped-pulse titanium–sapphire amplifier and with the frequency doubling BBO crystal in the nonlinear optical amplifier (NOPA), respectively. All samples were pumped at excitation densities between 1.14×10^9 and 1.90×10^9 W/cm^2.

The samples consisting of 1 mg of Ag clusters dispersed in 0.5 ml of absolute ethanol were irradiated in quartz cuvettes with a thickness of 2 mm. A fraction of the fundamental was simultaneously passed through a sapphire plate (3 mm) to generate the fs white-light continuum between 400 and 1400 nm. The chirp between 400 and 750 nm was approximately 350 fs. Transient absorption spectra of the Ag clusters in ethanol were taken at delay times between -0.5 ps and 4 ns. They were recorded in the visible region between 420 and 750 nm.

4. Results and Discussion

The Ag clusters were synthesized by reducing Ag^+ ions in acetonitrile at 75^{o}C and in DMF at 153^{o}C. However, to produce chemically stable, luminescent Ag clusters, the just formed clusters must be stabilized in time by suitable stabilizing agents. As stabilizing agent, we have used the biocompatible homopolymer poly(N-vinylpyrrolidone) (PVP) that contains an amide group in its monomeric unit and is known to have a good stabilizing ability for transition metal particles. The successful use of PVP as a stabilizing agent for the synthesis of Ag and Au clusters was already demonstrated by various other groups[19,45,46]. In the presence of PVP, the Ag^+ ions were chelated. Subsequent reduction of the Ag^+-PVP complexes by acetonitrile or DMF at the refluxing temperature of the respective solvent provided the formation of PVP-

stabilized Ag clusters. Remarkably, the same reduction reaction of Ag^{+}-PVP complexes, when performed at temperatures lower than the boiling point of the respective reducing agent and solvent, will yield large-sized Ag nanoparticles.

X-ray photoelectron spectroscopy (XPS) experiments were performed to examine the oxidation state of Ag in A-AgPVP clusters. The binding-energy values of 368.48 eV and 374.57 eV are assigned to $Ag3d_{5/2}$ and $Ag3d_{3/2}$ states, respectively (Figure 1.A). These values are very typical for elemental Ag (0) and therefore indicate the formation of ultrasmall Ag clusters. The binding energy of N1s and O1s were found to be 400.28 eV and 533.28 eV (Figures 1.B and C). The much larger binding energy value of the O1s orbital (533.4 eV) in the A-Ag-PVP clusters, when compared to that of the O1s orbital (531.3 eV) for the pure PVP sample, suggests efficient interactions between the oxygen atom of the monomer and surface Ag atoms. Such interactions between oxygen atom of the –C=O group of PVP and Ag atoms was also reported previously by Chen *et al.*[49].

TEM and HRTEM images of the Ag@PVP nanoparticles are shown in Figures 2.A and B. The Ag@PVP nanoparticles have a single-crystalline structure and an average size of 6.5 nm (Figure 2.D). However, because of their ultra-small sizes the Ag clusters could not be detected in TEM. The HRTEM image recorded at an accelerating voltage of 300 kV provides some clue about the formation of very small tiny clusters. An exemplary HRTEM image of the as-synthesized A-AgPVP clusters is depicted in Figure 2.C. The image shows some particles of which most of them have no definite shape. However we were able to resolve few spherical particles in the image which are marked by the red circle. The sizes of these spherical particles were estimated in the range of 1.3 nm to 1.5 nm. The HRTEM images histogram of the size distribution of the Ag@PVP nanoparticles is shown in Figure 2.D.

Figure 3 depicts the UV/Vis absorption spectra of the Ag clusters and Ag@PVP nanoparticles. The absorption spectrum of the Ag@PVP nanoparticles shows the characteristic surface plasmon resonance peak at 397 nm, whereas the absorption spectra of the Ag clusters do not contain this specific feature but consist of different, significantly structured, broad absorption bands. The A-AgPVP clusters exhibit weakly pronounced absorption peaks at 284 nm (4.36 eV), 350 nm (3.54 eV), 490 nm (2.53 eV), which are superimposed on a broad absorption background. On the other hand, the absorption spectrum of the D-AgPVP clusters contains a shoulder-like absorption feature around 350 nm. These absorption bands may be assigned to discrete electronic transitions between molecular-like

energy states and are therefore characteristic for clusters as essentially consisting of surface atoms. Recently, Zhang *et al*.[34] reported of a photo-activated synthesis of luminescent Ag clusters (Ag_4 – Ag_9) dispersed in polymer microgel which show a broad absorption band at 330-350 nm along with a peak at 490 nm in the UV/Vis absorption spectrum. Water soluble, luminescent Ag clusters stabilized by dihydrolipoic acid (DHLA) were observed to exhibit similar absorption features[17]. Several other research groups synthesized Ag clusters with various sizes using different capping agents, and for all clusters they found very similar absorption features in the UV and visible region of the spectrum[35,36,42,43,48]. In agreement with these results, the particular structural features of the absorption spectra may be associated with Ag clusters that consist of 5 to 9 atoms. Moreover, the UV/Vis absorption spectra of the as-synthesized Ag clusters did not change over a one-month storage time which proves their great stability.

The PVP concentrations play an important role in the formation of Ag clusters. When 0.075 M PVP (in terms of monomer unit) used in the reaction, luminescent Ag clusters stabilized by the PVP polymer were obtained. However, large-sized non-luminescent Ag nanoparticles were produced when small concentration of 0.025 M PVP was used in the reaction (Figure 4). Here in this reaction PVP acts as a cross-linking agent for clusters agglomeration. At high concentrations, the coil-like polymer cages encapsulated the clusters better and protected the clusters from quencher in solution. Moreover, a larger concentration of the stabilizer led to a smaller growth rate of the particles, and in turn facilitated the formation of clusters instead of nanoparticles. At low stabilizer concentrations, the reduction took place so fast that the polymer could not complex the silver ions in an efficient manner, which resulted in particle aggregation and consequently, large-sized nanoparticles were formed. Figure 4 shows the UV/Vis absorption spectra recorded after 5 h of the reaction between $AgNO_3$ and PVP in acetonitrile at reflux. For low PVP concentrations the formation of Ag nanoparticles is evident from the appearance of the surface plasmon resonance band at 405 nm in the UV/Vis absorption spectra.

Upon photoexcitation at 364 nm the A-AgPVP clusters emit a blue photoluminescence (PL) emission peaking at 424 nm (2.93 eV), while the PL emission spectrum of the D-AgPVP clusters is shifted into the spectral range around 450 nm (2.73 eV) (Figure 5). The corresponding PL excitation spectra exhibit their respective maximum at 350 nm (3.54 eV) for the A-AgPVP clusters and at 370 nm (3.35 eV) for the D-AgPVP clusters. The narrow PL emission profile indicates a small size distribution of the Ag clusters. The narrow size

distribution is also evident from the PL emission spectrum of the A-AgPVP clusters which was excited at different wavelengths ranging from 320 nm to 430 nm (Figure 6). Such shifting of the PL emission peak towards longer wavelengths with increasing excitation wavelengths indicates the presence of Ag clusters with different sizes. The linear dependence of the wavelength of the PL emission maximum on the PL excitation wavelength was already reported elsewhere[31,42,50] and is tentatively assigned to inter-band transitions from the sub-merged and quasi continuum 5d band to the lowest un-occupied conduction band states of Ag.

The PL emission maxima were observed to change relative to PVP concentration. Figure 7 shows the PL emission spectra of the A-AgPVP clusters prepared using different concentrations of PVP (0.075 M, 0.05 M, and 0.025M respectively). Clearly no luminescent Ag clusters were formed for a PVP concentration of 0.025 M. On the other hand, a slight red shift of the PL emission maximum was observed, when a threefold larger PVP concentration (0.075 M PVP) was used. Obviously PVP provides a cross-linking environment for the clusters so that the degree of this cross linking depends on the PVP concentration. Different concentrations of PVP impart different chemical and electronic environments for the clusters which results in different PL emission energies.

It has to be mentioned that neither the pure PVP solution nor solutions containing PVP with adsorbed or embedded Ag ions were found to emit detectable fluorescence under the same photo-excitation conditions. This unambiguously demonstrates that the observed PL has to be associated with the formation of reduced silver clusters embedded in a PVP matrix. Figure 8 depicts the reaction-time evolution of the PL emission spectra of A-AgPVP clusters. The reaction time of the A-AgPVP clusters corresponds to the duration of their synthesis when the reaction mixture was heated under reflux conditions. The PL emission was excited at 350 nm. Obviously, the PL intensity of Ag clusters increases with rising reaction time and reaches its maximum value for clusters synthesized over 5 hours refluxing. This implies that the reaction has come to an end after 5 hours refluxing time.

The PL quantum yields of the A-AgPVP and D-AgPVP clusters were determined using quinine sulphate as fluorescence standard, and the obtained values are $\Phi_{A\text{-}AgPVP}$ = 3.5 % and $\Phi_{D\text{-}AgPVP}$= 2.7 % respectively. Although reports on red-emitting Ag clusters are frequent, only few were published on blue-emitting Ag clusters. Recently, González *et al.* [44] developed an electrochemical synthesis procedure to synthesize blue-emitting and Ag_6 clusters that were stabilized with dodecanethiol and tetrabutyl ammonium. The Ag_6 clusters exhibit PL emission around 420 nm with a quantum yield of 1.2 %. The PL emission spectrum of these Ag clusters

nicely coincides with that of the here synthesized A-AgPVP clusters, whereas the PL quantum yield is significantly smaller than that of the A-AgPVP clusters with a value of 3.5 %. Furthermore, Ag clusters stabilized with polyethyleneimine polymer were reported to emit PL in the range of 420 – 490 nm [44,51,52].

The A-AgPVP clusters show great chemical stability towards various kinds of solvents. To examine the colloidal stability of these clusters, their PL emission spectrum was measured in aqueous solution at different pH values and in an aqueous solution with a high ionic strength (0.5 M NaCl). Almost the same PL emission intensity of the A-AgPVP clusters was observed under all solvent conditions and that even after 14 days of preparation (Figures 9A, B and C). These results suggest the high chemical stability of the A-AgPVP clusters in acidic and basic solvents as well as in solution with high ionic strengths. Strikingly, the addition of NaCl to the solvent is associated with small red shift of the PL emission maximum of the A-AgPVP clusters. Moreover, the addition of a reducing agent such as $NaBH_4$ or of an oxidizing agent like H_2O_2 to the A-AgPVP cluster colloid was not observed to alter the spectral features of their PL emission and UV/Vis absorption spectra. These experimental results prove both, the high stability of the Ag clusters and the absence of any Ag^+ ions in the solution.

PL lifetime measurements of the A-AgPVP and D-AgPVP clusters were performed by detecting their PL emission at 430 nm and 450 nm, respectively. The PL emission decay curves were simulated employing a convolution of the apparatus response with a bi-exponential decay function f(t) being $f(t)= a_1\times\exp(-t/\tau_1) + a_2\times\exp(-t/\tau_2)$ (Figure 10). For the A-AgPVP clusters, the predominant slow decay component, with $a_2= 0.7$ and $\tau_2= 2.5$ ns is assigned to the PL emission decay of Ag_6 clusters, whereas the larger time constant ($\tau_2= 3.4$ ns, $a_2= 0.6$) of the D-AgPVP clusters is assigned to the lifetime of the emitting state of Ag_7 clusters. The respective faster PL emission decay component of the A-AgPVP and D-AgPVP clusters ($\tau_1= 0.4$ ns or 0.6 ns) might reveal the contribution to the PL emission due to smaller Ag clusters.

Complementary information of ultrafast excited-state relaxation dynamics of A-AgPVP clusters was obtained from fs transient absorption spectroscopy experiments. Figure 11 presents the time evolution of the transient absorption spectra of the excited-state relaxation dynamics of the Ag clusters following excitation at 387 nm. The spectra exhibit a broad featureless photo-induced absorption signature between 450 and 700 nm with a maximum around 570 nm. The short-time scale kinetic traces detected at 510 and 570 nm display the temporal decay behavior of the overall transient absorption spectrum. The kinetic traces were

fit using a bi-exponential function that is deconvolved with a 240 fs Gaussian representing the apparatus response. The bi-exponential decay dynamics comprises a subpicosecond (65 %) and a picosecond decay component (35 %). The ultrashort lifetime with τ_1= 0.3 ps is attributed to internal conversion as being the process that provides ultrafast relaxation dynamics of initially photo-excited, higher electronic states to the S_1 state. On the other hand, the larger time constant with τ_2= 3.3 ps is associated with surface trapping of the initially generated excitons.

4. Conclusions

In summary, a novel synthesis route was developed which was successfully used to prepare highly luminescent, stable and nearly mono-disperse Ag clusters. Our synthesis recipe consists in a facile, environmentally friendly on-step reaction, in which PVP acts as the stabilizing agent and acetonitrile or DMF serve as both, solvent and reducing agent. The XPS results confirm the complete reduction of silver ions and furthermore, verify efficient interactions between the oxygen atom of the monomer unit and the Ag cluster. The PL lifetimes of the A-AgPVP clusters and D-AgPVP clusters were determined with 2.5 ns and 3.4 ns, respectively. For the A-AgPVP clusters, fs transient absorption spectroscopy experiments allowed for the observation of bi-exponential ultrafast excited-state relaxation dynamics. The two obtained time constants with 0.3 ps and 3.3 ps were assigned to ultrafast internal conversion emerging from initially higher-lying energy states to the emitting S_1 state and surface capturing of the photo-generated charge carriers. In accord with the actual literature, our evaluated spectroscopic and microscopic results suggest that this synthesis technique predominantly produces ultra-small fluorescent silver clusters having less than 10 atoms in the core.

5. References

1. M. Haruta, *Chem. Rev*. 2003, 3, 75.
2. L. Li, Q. Guo, J. Li, W. Yan, C. Leng, H. Tang, Q. Lu and B. Tan, *J. Mater. Chem. B*, 2013, 1, 3999.
3. J. Zheng, P. R. Nicovich and R. M. Dickson, *Annu. Rev. Phys. Chem*., 2007, 58, 409.
4. B. H. Kim, M. J. Hackett, J. Park and T. Hyeon, *Chem. Mater.*, 2014, 26, 59.
5. S. Parween, A. Ali and V. S. Chauhan, *ACS Appl. Mater. Interfaces*, 2013, 5, 6484.
6. R. A. Sperling, P. Rivera Gil, F. Zhang, M. Zanella and W. J. Parak, *Chem. Soc. Rev*., 2008, 37, 1896.

7. X. Wu, X. He, K. Wang, C. Xie, B. Zhou and Z. Qing, *Nanoscale*, 2010, 2, 2244.
8. S. K. Rastogi, V. J. Rutledge, C. Gibson, D. A. Newcombe, J. R. Branen and A. L. Branen, *Nanomed. Nanotechnol. Biol. Med*., 2011, 7, 305.
9. T. H. Lee, J. I. Gonzalez, J. Zheng and R. M. Dickson, *Acc. Chem. Res*., 2005, 38, 534.
10. T. G. Schaaff and R. L. Whetten, *J. Phys. Chem. B*, 2000, 104, 2630.
11. C. B. Murray, D.J. Norris and M. G. Bawendi, *J. Am. Chem. Soc*. 1993, 115, 8706.
12. W. C. W. Chan and S.Nie, *Science*, 1998, 281, 2016.
13. Y. G. Sun and Y.Xia, *Science*, 2002, 298, 2176
14. T. Zhou, M. Rong, Z. Cai, C. James Yang and X. Chen, *Nanoscale*, 2012, 4, 4103.
15. M. C. Pau, C. K. Lo, X. Yang and M. M. F. Choi, *J. Phys. Chem. C*, 2010, 114, 15995.
16. J. Sun, J. Zhang and Y. Jin; *J. Mater. Chem. C*, 2013, 1, 138.
17. B. Adhikari and A. Banerjee, *Chem. Mater*., 2010, 22, 4364.
18. C. A. J. Lin, T. Y. Yang, C. H. Lee, S. H. Huang, R. A. Sperling, M. Zanella, J.K. Li, J. L. Shen, H. H. Wang, H. I. Yeh, W. J. Parak, and W. H. Chang, *ACS Nano*, 2009, 3, 395.
19. H. Tsunoyama, N. Ichikuni, H. Sakurai and T. Tsukuda, *J. Am. Chem. Soc.*, 2009, 131, 70.
20. J. Zheng and R. M. Dickson, *J. Am. Chem. Soc.* 2002, 124, 13982.
21. J. Sharma, R. C. Rocha, M. L. Phipps, H.-C. Yeh, K. A. Balatsky, D. M. Vu, A. P. Shreve, J. H. Werner and J. S. Martinez, *Nanoscale*, 2012, 4, 4107.
22. N. Makarava, A. Parfenov and I. V. Baskakov, *Biophys. J.*, 2005, 89, 572.
23. M. Scolari, A. Mews, N. Fu, A. Myalitsin, T. Assmus, K. Balasubramanian, M. Burghard and K. Kern, *J. Phys. Chem. C*, 2008, 112, 391.
24. Z. Shen, H. W. Duan and H. Frey, *Adv. Mater.*, 2007, *19*, 349.
25. F. Qu, N. Bing Li and H. Qun Luo, *J. Phys. Chem. C*, 2013, 117, 3548.
26. C. Guo, and J. Irudayaraj, *Anal. Chem.*, 2011, 83, 2883.
27. J. Xie , Y. Zheng and J. Y. Ying, *J. Am. Chem. Soc.*, 2009, 131, 888.
28. J. T. Petty, J. Zheng, N. V. Hud and R. M. Dickson, *J. Am. Chem. Soc.,* 2004, 126, 5207.
29. W. W. Guo, J. P. Yuan and E. K. Wang, *Chem. Commun.*, 2009, 3395.
30. C. I. Richards, S. Choi, J. C. Hsiang, Y. Antoku, T. Vosch, A. Bongiorno, Y. L.Tzeng and R. M. Dickson, *J. Am. Chem. Soc.*, 2008, 130, 5038.
31. L. Shang and S. J. Dong, *Chem. Commun.*, 2008, 1088.
32. J. Zheng and R. M. Dickson, *J. Am. Chem. Soc.*, 2002, 124, 13982.
33. J. Zheng, J. T. Petty and R. M. Dickson, *J. Am. Chem. Soc.*, 2003, 125, 7780.
34. J. G. Zhang, S. Q. Xu, E. Kumacheva, *Adv. Mater.*, 2005, 17, 2336.

35. K. V. Mrudula, T. Udaya Bhaskara Rao and T. Pradeep, *J. Mater. Chem*., 2009, 19, 4335.
36. M. Farrag, M. Thämer, M. Tschurl, T. Bürgi and U. Heiz, *J. Phys. Chem. C,* 2012, 116, 8034.
37. L.A. Peyser, A. E. Vinson, A. P. Bartko and R. M. Dickson, *Science*, 2001, 291,103.
38. J. Sharma, H.-C. Yeh, H. Yoo, J. H. Werner and J. S. Martinez, *Chem.Comm*, 2011, 47, 2294.
39. L. Shang, R. M. Dörlich, S. Brandholt, R. Schneider, V. Trouillet, M. Bruns, D. Gerthsen and G. U. Nienhaus, *Nanoscale*, 2011, 3, 2009.
40. S. Huang, C. Pfeiffer, J. Hollmann, S. Friede, J. Jin-Ching Chen, A. Beyer, B. Haas, K. Volz, W. Heimbrodt, J. M. Montenegro Martos, W. Chang and W. J. Parak, *Langmuir*, 2012, 28, 8915
41. A. Henglein, *J. Phys. Chem.,* 1993, 97, 5457.
42. S. Liu, F. Lu and J.-J. Zhu, *Chem. Commun.*, 2011, 47, 2661.
43. H. Xu and K. S. Suslick, *ACS Nano*, 2010, 4, 3209.
44. B. S. González, M. C. Blanco and M. Arturo López-Quintela, *Nanoscale*, 2012, 4, 7632.
45. I. Pastoriza-Santos and L. M. Liz-Marzán, *Langmuir*, 1999, 15, 948.
46. I. Pastoriza-Santos and L. M. Liz-Marzán, *Langmuir*, 2002, 18, 2888.
47. X. Liu, C. Li, J. Xu, J. Lu, M. Zhu, Y. Guo, S. Cui, H. Liu, S. Wang and Y. Li, *J. Phys. Chem. C*, 2008, 112, 10778.
48. N. Cathcart and V. Kitaev, *J. Phys. Chem. C*, 2010, 114, 16010.
49. B. Yin, H. Ma, S. Wang and S. Chen, *J. Phys. Chem. B*, 2003, 107, 8898.
50. I. Diez, M. I. Kanyuk, A. P. Demchenko, A. Walther, H. Jiang, O. Ikkala and R. H. A. Ras, *Nanoscale*, 2012, 4, 4434
51. F. Qu, L. L. Dou, N. B. Li and H. Q. Luo, *J. Mater. Chem* C, 2013, 1, 4008.
52. N. Y. Chen, H. F. Li, Z. F. Gao, F. Qu, N. B. Li, H. Q. Luo, *Sensors and Actuators B: Chemical*, 2014, 193, 730.

Figures:

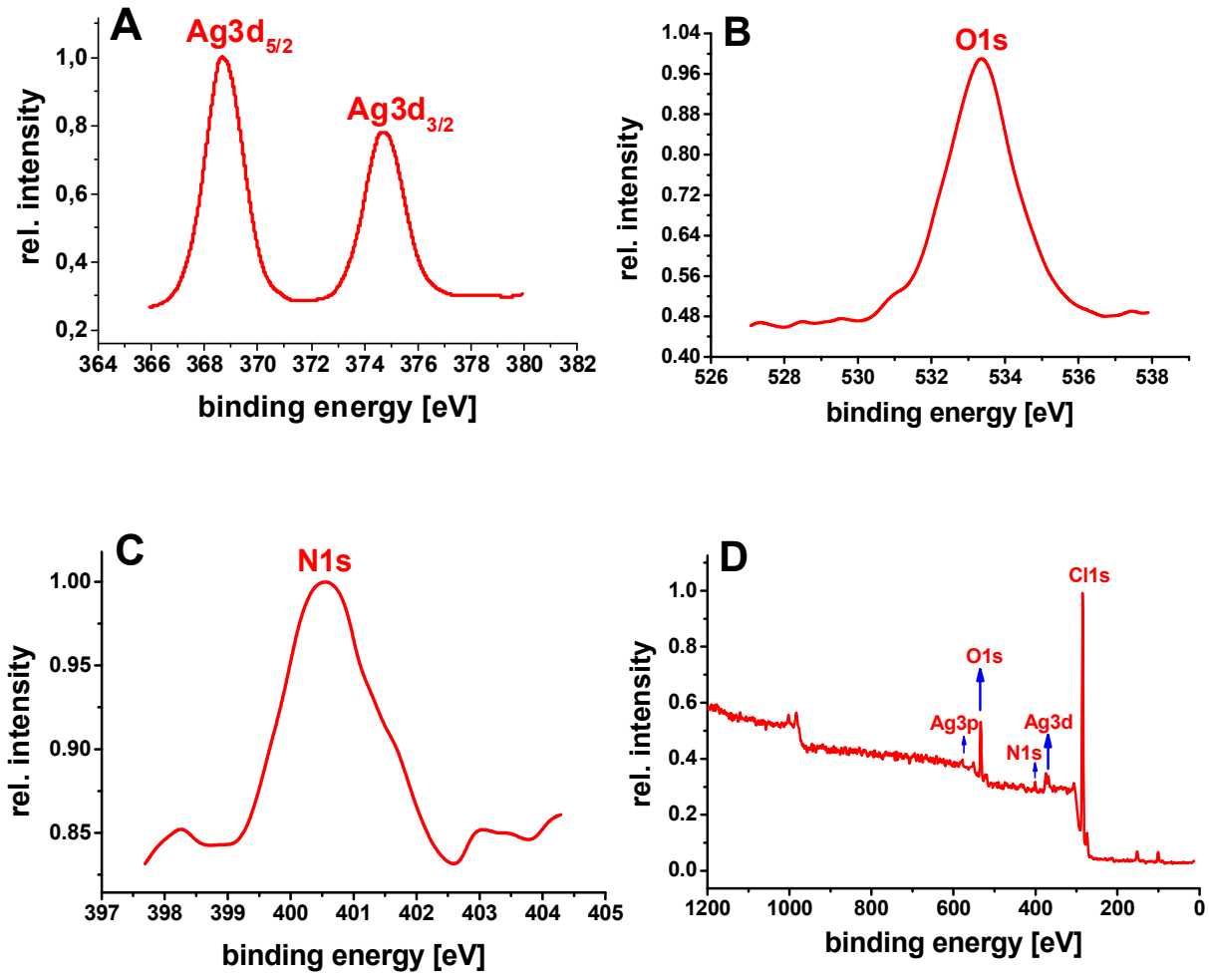

Figure 1:

A, B, and C are the XPS spectra of Ag3d, O1s and N1s regions of the A-AgPVP clusters respectively; the survey XPS spectra of the A-AgPVP clusters is depicted in D.

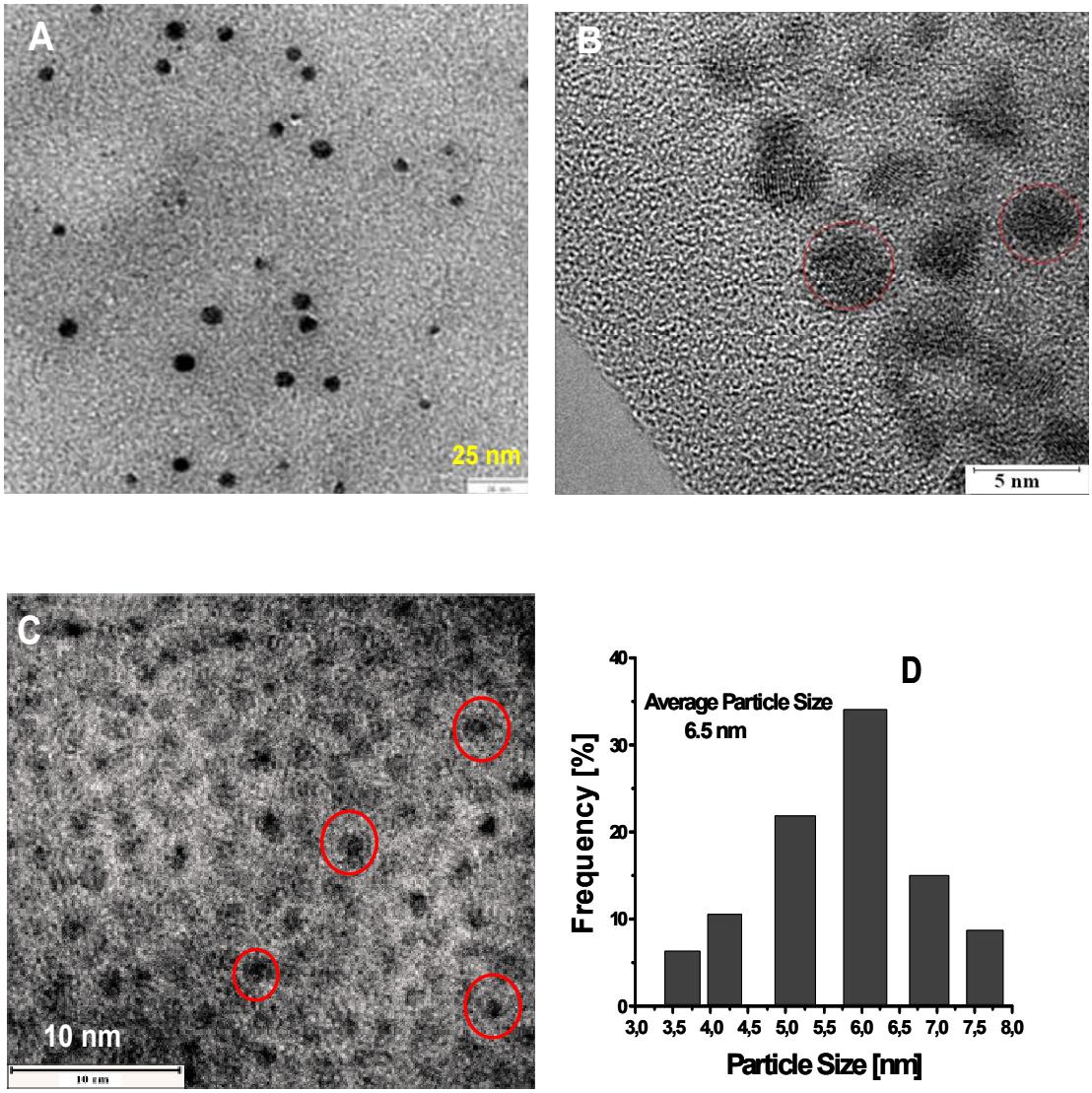

Figure 2:

TEM image of the Ag@PVP nanoparticles (A); HRTEM images of the Ag@PVP nanoparticles (B) and A-AgPVP clusters (C); D represents the HRTEM images histogram of the size distribution of the Ag@PVP nanoparticles.

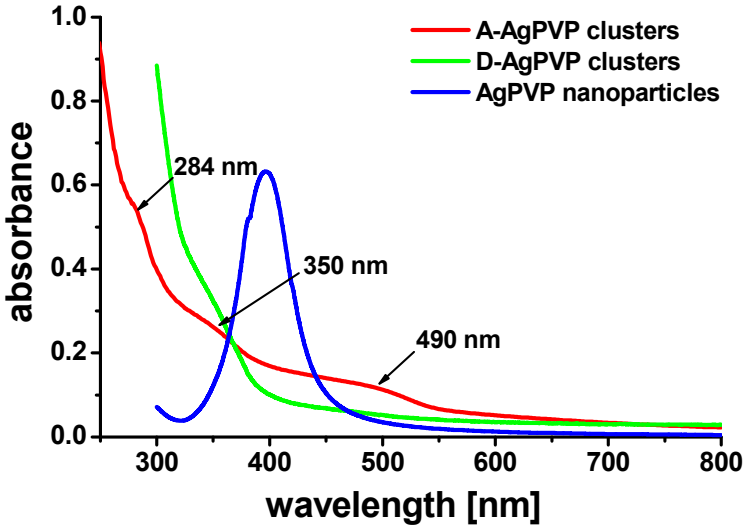

Figure 3:

UV/Vis absorption spectra of the as-synthesized A-AgPVP clusters (red solid line), D-AgPVP clusters (green solid line) and Ag@PVP nanoparticles (blue solid line).

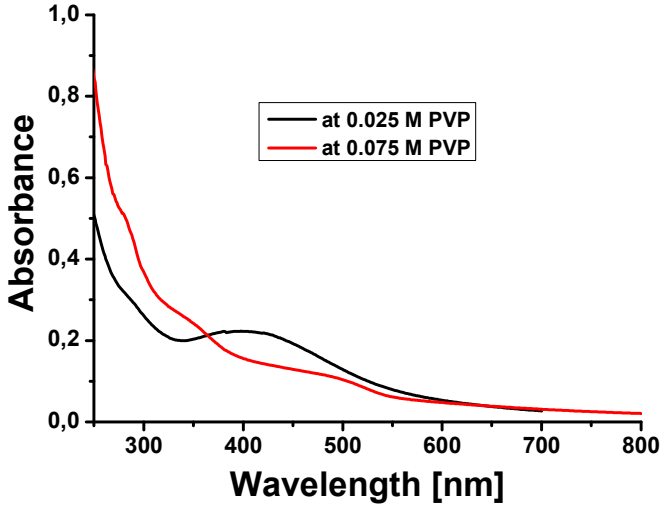

Figure 4 :

UV/Vis absorption spectra recorded after 5 h of reaction between $AgNO_3$ and PVP solution in acetonitrile at reflux. The PVP concentrations used are 0.075 M (red solid line) and 0.025 M (black solid line).

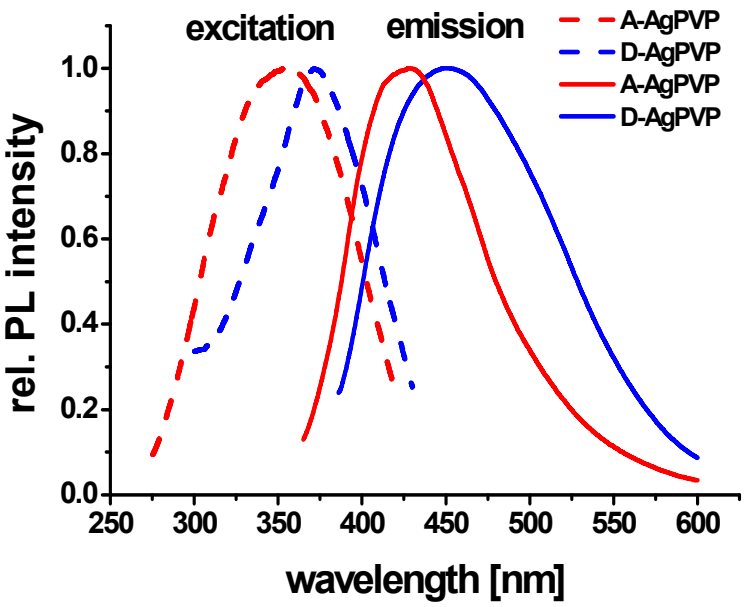

Figure 5:

PL excitation spectra of the A-AgPVP clusters (red dashed line) and D-AgPVP clusters (blue dashed line) and PL emission spectra of the A-AgPVP clusters (red solid line) and D-AgPVP clusters (blue solid line).

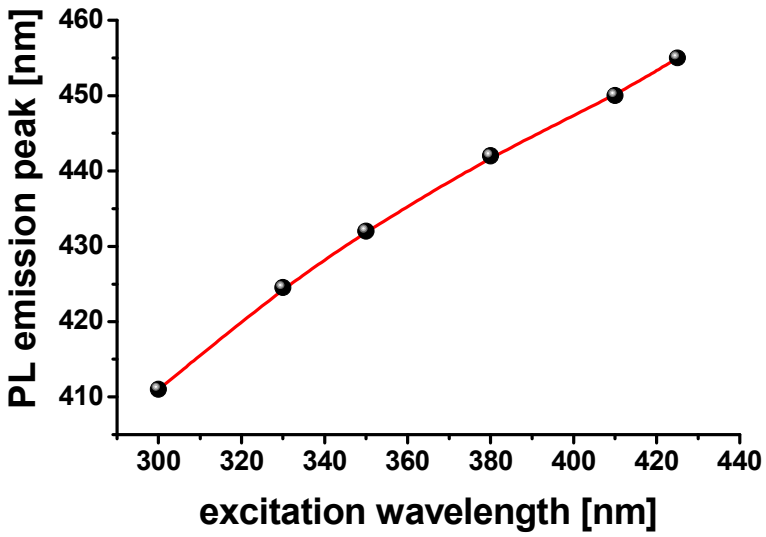

Figure 6:

The dependence of the PL emission peaks of the A-AgPVP clusters on the excitation wavelength.

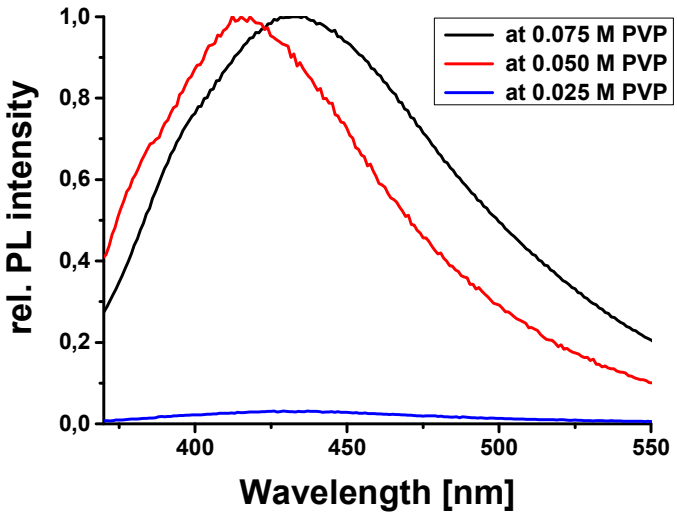

Figure 7:

PL emission spectra of the A-AgPVP clusters synthesized using various concentrations of PVP; 0.075 M (black solid line), 0.050 M (red solid line) and 0.025 M (blue solid line) respectively.

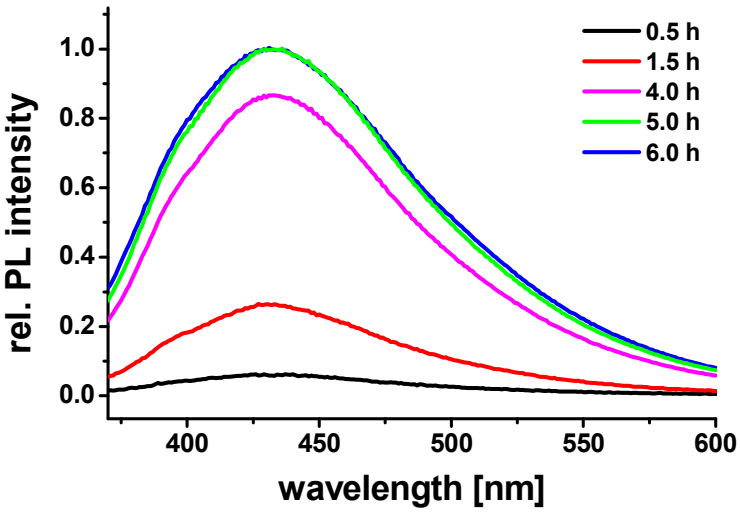

Figure 8:

PL emission spectra of the as-synthesized A-AgPVP clusters excited at 350 nm and recorded at different reaction times.

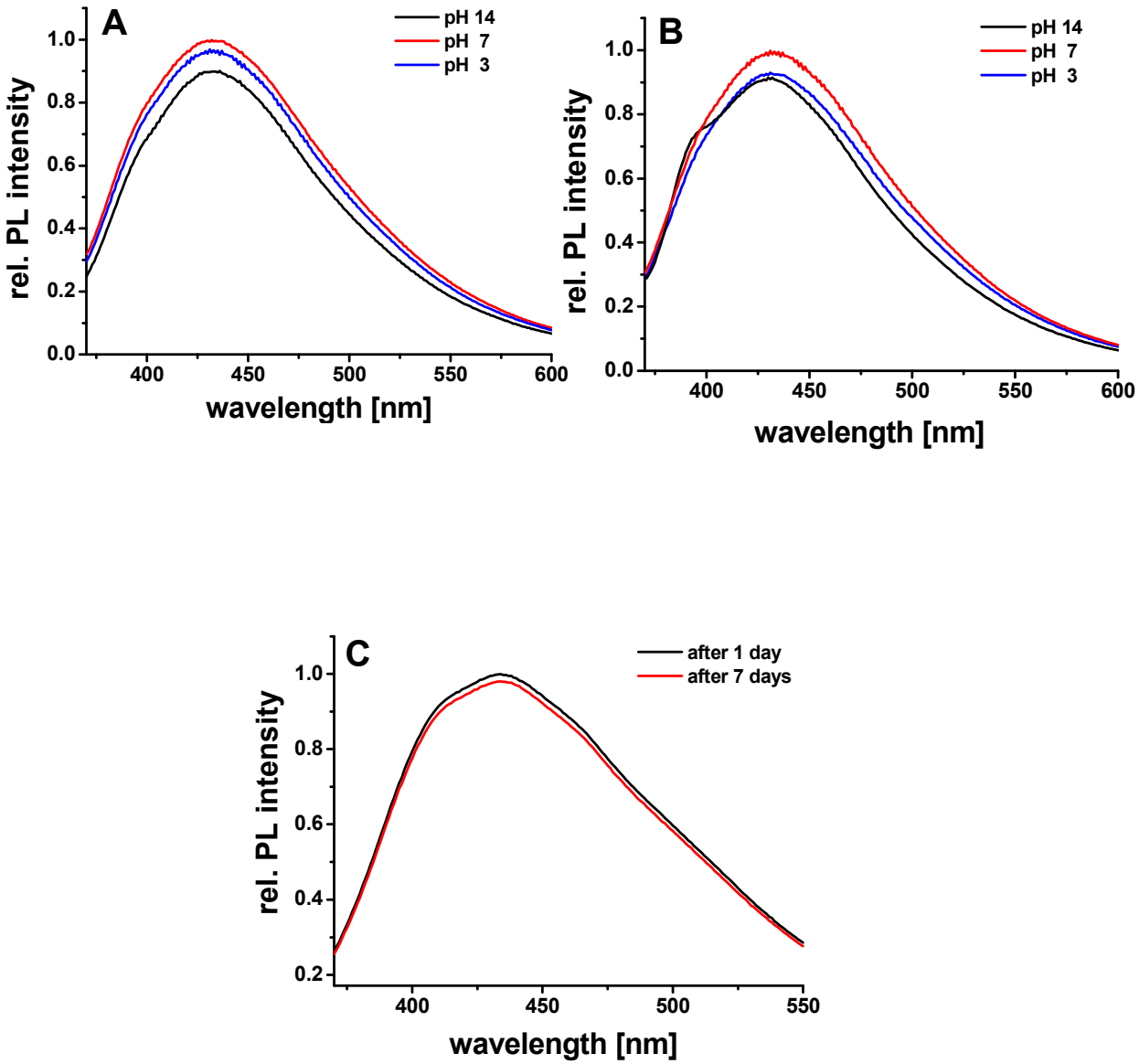

Figure 9:

PL emission spectra of A-AgPVP clusters in an aqueous solution at pH values of 3, 7 and 14 after 7 days (A) and 14 days (B) of preparation; PL emission spectra of the A-AgPVP clusters in a 0.5 M NaCl aqueous solution after 7 and 14 days of preparation (C).

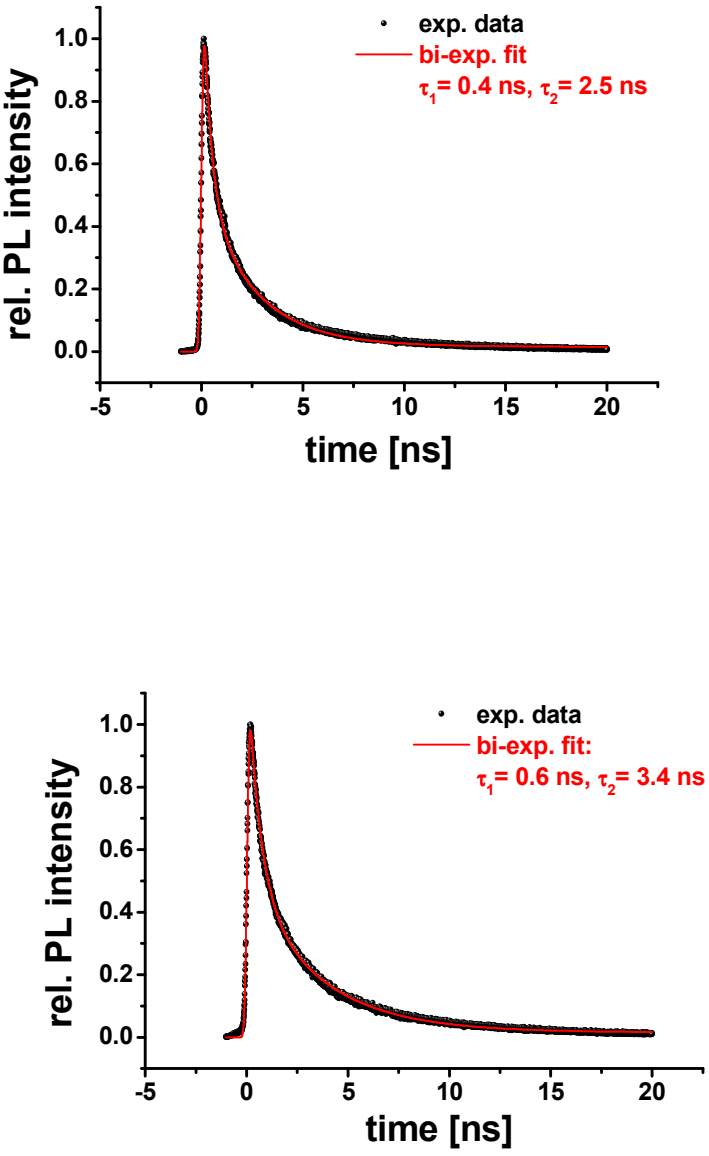

Figure 10:

PL emission decays of the A-AgPVP clusters (at top) and the D-AgPVP clusters (at bottom), both excited at 403 nm.

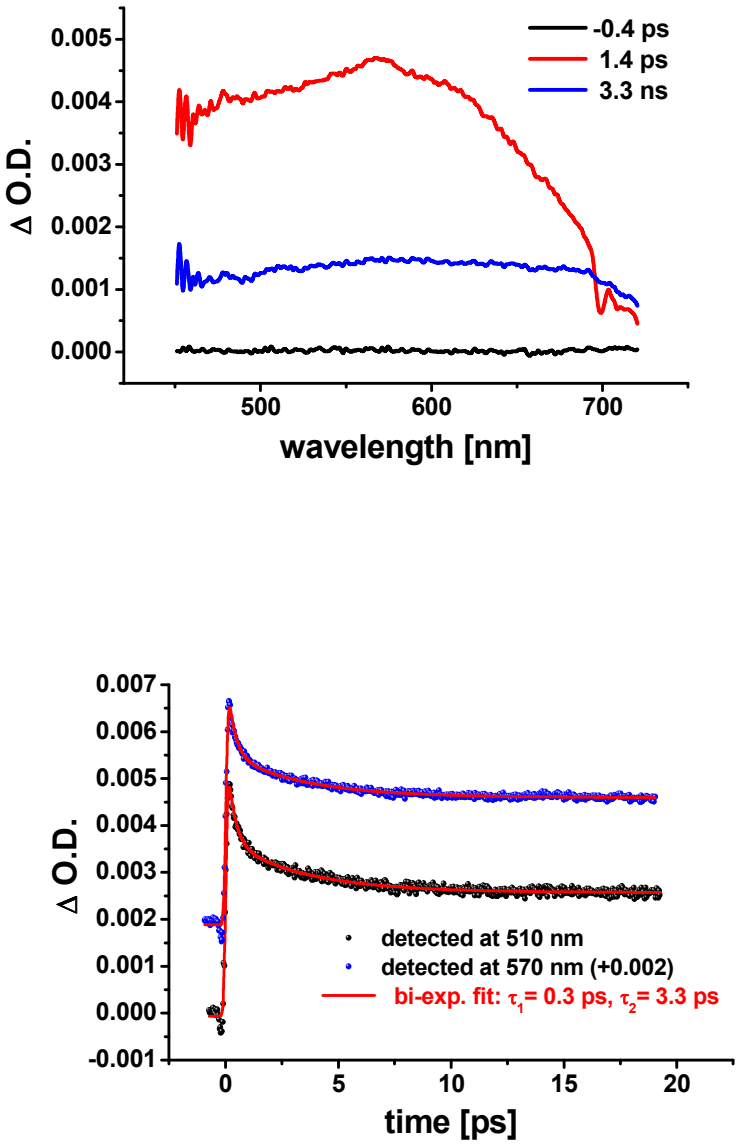

Figure 11:

Time evolution of the transient absorption spectra (at top) with their characteristic kinetic traces (at bottom) of the A-AgPVP clusters.